JOURNAL OF NANO- AND ELECTRONIC PHYSICS
Vol. **18** No 3, 03025(4pp) (2026)

ЖУРНАЛ НАНО- ТА ЕЛЕКТРОННОЇ ФІЗИКИ
Том **18** № 3, 03025(4cc) (2026)

OPEN ACCESS

REGULAR ARTICLE

Optimization of Various Physical Properties of a $CsPbI_{3-X}Br_X$ ($X = 0, 1$)-Based Perovskite Solar Cell

Kunal Chakraborty[1,*], R. Narmadha[2,†], Islom Kadirov[3], Visalakshi Naraparedddi[4], M. Lakshmu Naidu[5], Karedla Chitambara Rao[6]

[1] *Department of Electrical Engineering, IMPS College of Engineering and Technology, Malda, West Bengal, India*
[2] *Department of Mechatronics, Sathyabama Institute of Science and Technology, Chennai, Tamil Nadu, India*
[3] *Department of Transport Systems, Urgench State University, Urgench, Uzbekistan*
[4] *School of Business, Aditya University, Aditya Nagar, ADB Rd, 533437 Surampalem, Andhra Pradesh, India*
[5] *Department of Electronics and Communication Engineering, Koneru Lakshmaiah Education Foundation, Vaddeswaram, 522302 Guntur, Andhra Pradesh, India*
[6] *Department of Electronics and Communication Engineering, Aditya Institute of Technology and Management, 532203 Tekkali, Andra Pradesh, India*

(Received 27 February 2026; revised manuscript received 21 June 2026; published online 26 June 2026)

Perovskite solar cells are the most promising alternative sources of clean energy. In this re-search work, a regular Cs-based halide ($CsPbI_3$) and mixed halide ($CsPbI_2Br$) PSC were developed to study the thickness, device temperature, and material defect density using the SCAPS-1D simulator under an ideal 27 °C ambient temperature. In this device model, TiO_2 and CuSCN are used as ETL (electron transport layer) and HTL (hole transport layer), and FTO and Ag are used as front and back electrodes, respectively. The structure of the device is the *n-i-p* type FTO/TiO_2/$CsPbI_3$/CuSCN/Ag and FTO/TiO_2/$CsPbI_2Br$/CuSCN/Ag-based halide and mixed halide model. The optimized thickness of the halide ($CsPbI_3$) and mixed halide ($CsPbI_2Br$)-based PSC is 500 nm. The optimal conversion efficiency for the FTO/TiO_2/$CsPbI_3$/CuSCN/Ag and FTO/TiO_2/$CsPbI_2Br$/CuSCN/Ag-based halide and mixed halide PSC is 11.07 % and 10.89 %, respectively. The V_{OC} of the halide ($CsPbI_3$) and mixed halide ($CsPbI_2Br$)-based PSC at maximum power point is 1.21 V and 0.84 V. The optimal device temperature and material defect density for the halide ($CsPbI_3$) and mixed halide ($CsPbI_2Br$)-based PSC are 30 °C and 10^{12} cm^{-3}, respectively.

Keywords: $CsPbI_3$, $CsPbI_2Br$, Perovskite, SCAPS-1D, Thickness, PCE.

DOI: 10.21272/jnep.18(3).03025 PACS number: 88.40.jm, 88.40.H –

1. INTRODUCTION

The rise in energy demand in the modern era has uplifted the new energy sources like renewable energy to produce clean electricity [1-4]. In the category of renewable energy sources, solar energy is the most desirable alternative. Solar energy is one of the simplest energy sources, where sunlight is directly converted into electricity. The microscopic attributes of solar cell materials and the advancement of new techniques have created modern high-performance solar cells [1-7]. One of the significant achievements that have received great attention since the past decade is the perovskite solar cell (PSC)-based photovoltaic (PV) device [8]. These solar cell materials have great physical, optical, electronic, and mechanical properties [8-9]. Besides those advantages, the PSCs have low production costs and a simple production process [10-11]. The conversion efficiency of the PSC-based device rises from 3.8 % to 25 % and above [1, 12-15]. The higher conversion efficiency was achieved from the hybrid device structure. This type of PSC device model consists of a front electrode, *n*-ETM (electron transport material), absorbing layer, *p*-HTM (hole transport material), and back electrode [16-17]. These hybrid model PSCs have power conversion efficiency almost near to the thin-film-based solar cells.

Our research work focuses on a simulation-based study to analyze the PV performance of FTO/TiO_2/$CsPbI_3$/CuSCN/Ag and FTO/TiO_2/$CsPbI_2Br$/CuSCN/Ag-based halide and mixed halide models. All the physical properties of the absorbing layer, including the thickness of $CsPbI_3$ and $CsPbI_2Br$-based PSC, and their defects were studied under optimal conditions. Later, the temperature of the device under optimized thickness of PSC is studied.

2. DEVICE STRUCTURE AND SIMULATION

The regular planar module of the proposed PSC device is divided into two structures: FTO/TiO_2/$CsPbI_3$/CuSCN/Ag and FTO/TiO_2/$CsPbI_2Br$/CuSCN/Ag-based halide and mixed halide models. The schematic diagram of the proposed device model is depicted in Fig. 1.

* Correspondence e-mail: kunal.eiilm.vu@gmail.com
† narmadhar2014om@gmail.com

Cite this article as: K. Chakraborty et al., *J. Nano- Electron. Phys.* 18 No 3, 03025(2026) https://doi.org/10.21272/jnep.18(3).03025

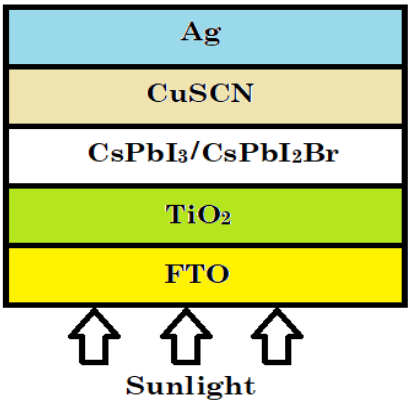

Fig. 1 – Schematic diagram of the proposed device model

The entire simulation process was executed in the SCAPS workstation. All the required device parameters used for that study were taken from various reported articles, and they are mentioned in Table 1 [8, 18-20].

Table 1 – Details of various device parameters

Parameters	Cs_2PbI_3	Cs_2PbI_2Br	TiO_2	CuSCN
λ (nm)	350	350	50	25
E_g (eV)	1.78	1.88	3.2	3.4
E_a(eV)	3.49	3.73	4.1	1.9
ζ_r	6	8.6	9	10
μ_n (cm^2/vs)	16	25	20	2×10^{-4}
μ_h (cm^2/vs)	16	25	10	2×10^{-1}
N_D (cm^{-3})	0	0	1×10^{19}	0
N_A (cm^{-3})	1×10^{15}	1×10^{15}	0	3×10^{18}

Our research work showed the effect of physical properties, including active layer thickness, device temperature, and material defect density, on the device performance. Here, λ, E_g, E_a, N_D, N_A, μ_n and μ_h are defined as thickness, band gap, electron affinity, relative permittivity, donor density, acceptor density, electron mobility, and hole mobility, respectively [8]. The energy-level diagram of the FTO/TiO_2/$CsPbI_3$/CuSCN/Ag- and FTO/TiO_2/ $CsPbI_2Br$/CuSCN/Ag-based PSC is depicted in Fig. 2.

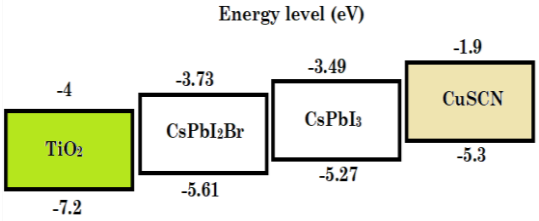

Fig. 2 – Energy level diagram of the proposed device model

3. RESULTS AND DISCUSSION

3.1 Active Layer Thickness Optimization

In this section, physical properties of the active layer, viz., the thickness of $CsPbI_3$ and $CsPbI_2Br$-based PSC materials, were varied from 100 nm to 900 nm to find the optimized thickness where the PV performance of the device is maximum. All the parameters of device materials are taken from Table 1. Here, Fig. 3 and Fig. 4 represent the V_{OC} and PCE changes with the thickness graph of the FTO/TiO_2/$CsPbI_3$/CuSCN/Ag and FTO/TiO_2/$CsPbI_2Br$/CuSCN/Ag-based PV devices. Fig. 3 and Fig. 4 showed that with every increment in thickness of the active layer, both the device PV parameters V_{OC} and PCE increase initially up to 500 nm thickness, and after 500 nm thickness, both those PV parameters decrease gradually. The main reason for that incident is that at higher thicknesses the absorption of light intensity is higher, and as a result, more charge carriers are generated [8, 20]. But higher light absorption is also responsible for heat production in the device, which leads to a drop in V_{OC} and PCE. Thus, 500 nm thickness will be the optimized thickness for those $CsPbI_3$– and $CsPbI_2Br$-based PSC materials. At 500 nm thickness, the PV performance of FTO/TiO_2/$CsPbI_3$/CuSCN/Ag and FTO/TiO_2/ $CsPbI_2Br$/CuSCN/Ag-based PV devices is reported in Table 2.

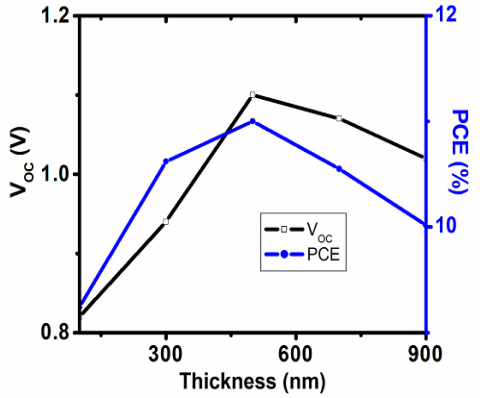

Fig. 3 – Variation of V_{OC}, PCE with the thickness of $CsPbI_3$

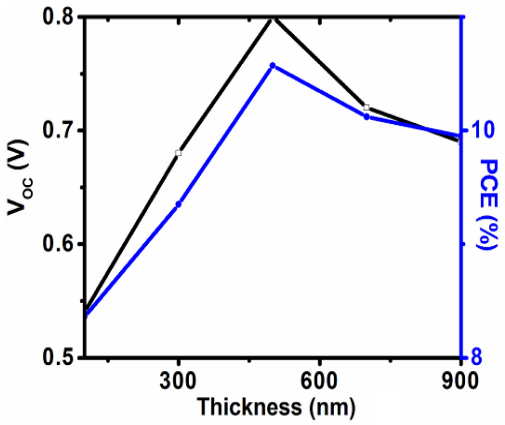

Fig. 4 – Variation of V_{OC}, PCE with the thickness of $CsPbI_2Br$

Here, the PV performance parameters are open circuit voltage (V_{OC}), short circuit current density (J_{sc}), power conversion efficiency (PCE), and fill factor (FF), respectively.

Table 2 – PV performance of the PSC

Materials	V_{OC} (V)	J_{SC} (mA/cm^2)	PCE (%)	FF (%)
Cs_2PbI_3	1.21	13.09	11.07	64.66
Cs_2PbI_2Br	0.84	15.93	10.89	78.32

3.2 Effect of Device Temperature

Device temperature optimization is an important study in the PSC simulation.

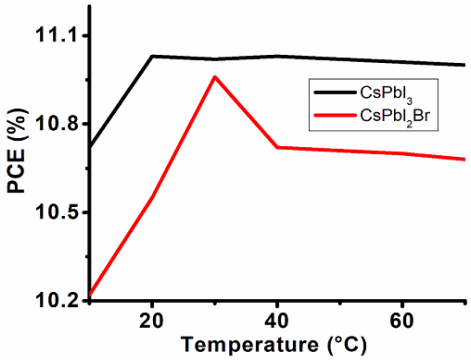

Fig. 5. Effect of temperature on device performance

The temperature of the device changes from 10 °C to 70 °C. The PCE-temperature plot is shown in Fig. 5. From that figure it is clearly observed that the PCE of both the FTO/TiO_2/$CsPbI_3$/CuSCN/Ag- and FTO/TiO_2/$CsPbI_2Br$/CuSCN/Ag-based PV devices increases initially up to 30 °C temperature. After that temperature, there is no significant change in PCE observed for either device. Higher temperature may lead to a drop in V_{OC}, and as a result, PCE also decreases.

3.3 Effect of Defect Density

Defect density (N_t, cm^{-3}) played an important role towards the PV performance of a PSC material. Here, Fig. 6 shows the PCE-N_t plot of the $CsPbI_3$– and $CsPbI_2Br$-based PSC material. It is impossible to neglect defects from the PSC material. From Fig. 6, it is clear that up to 10^{12} cm^{-3} N_t, the PCE of the FTO/TiO_2/$CsPbI_3$/CuSCN/Ag and FTO/TiO_2/ $CsPbI_2Br$/CuSCN/Ag-based PV device increases. After 10^{12} cm^{-3} defect density, the PCE of the device decreases significantly. So, the optimized defect density for $CsPbI_3$- and $CsPbI_2Br$-based PSC material is 10^{12} cm^{-3}.

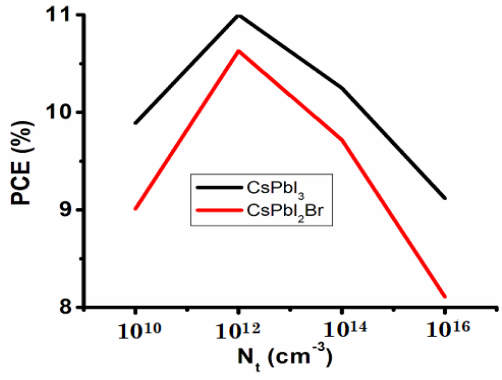

Fig. 6 – Effect of defect density on device performance

3.4 Recombination Study

Recombination study played important role to understand the rate of loss of photogenerated charge before it converted into current. Here, Fig. 7 shows the total recombination current (J_r, mA/cm^2) and Shockley-Read-Hall current (J_{SRH}, mA/cm^2) plot of the FTO/TiO_2/$CsPbI_3$/CuSCN/Ag and FTO/TiO_2/ $CsPbI_2Br$/CuSCN/Ag-based PV device. From this graph it is clear that as the voltage increases both the J_r and J_{SRH}, initially remained almost constant up to 0.6 V. After that 0.6 V both the J_r and J_{SRH} increases abruptly.

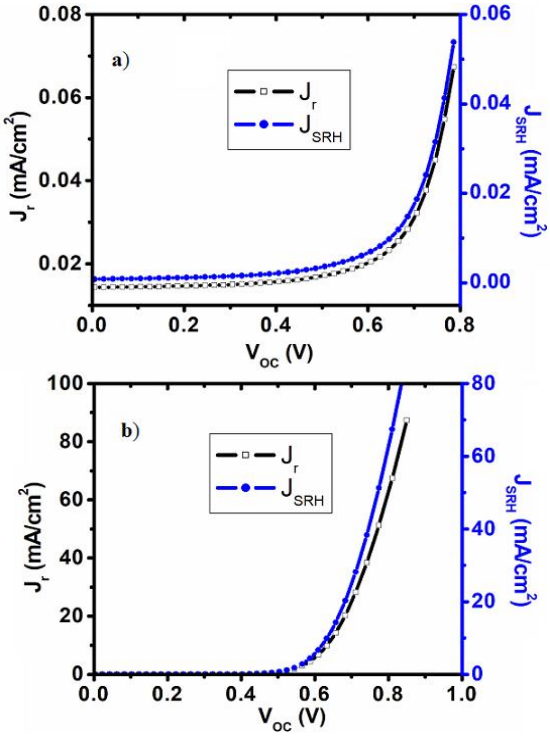

Fig. 7 – Recombination plot: a) $CsPbI_3$, b) $CsPbI_2Br$

3.5 Power Density Study

Here, Fig. 8 shows the power density plot of the device.

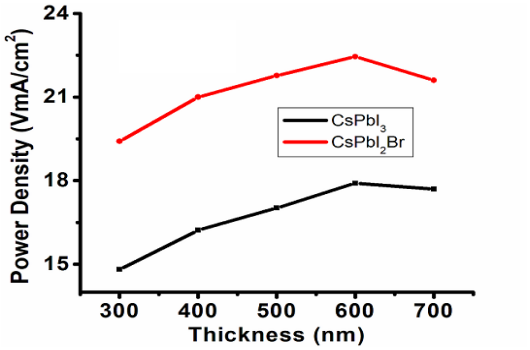

Fig. 8 – Power density plot of the device

From this figure it is clear that up to 600 nm thickness the power density of the device is increases significantly and after that thickness the power density started to decrease. The main reason behind that incident is the recombination rate increases with higher thickness of active layer.

4. CONCLUSION

This research work showed the PV performance analysis of a halide ($CsPbI_3$) and mixed halide (CsP-

bI$_2$Br) PSC using a SCAPS-1D simulator. Various physical properties, including the thickness of halide (CsPbI$_3$) and mixed halide (CsPbI$_2$Br) PSCs, followed by their defect density study and device temperature analysis. The PCE of halide (CsPbI$_3$) and mixed halide (CsPbI$_2$Br) PSCs at the maximum power point is 11.07 % and 10.89 %. Similarly, the V_{OC} of halide (CsPbI$_3$) and mixed halide (CsPbI$_2$Br) PSC is 1.21 V and 0.84 V, respectively. The optimized device temperature and material defect density for the halide (CsPbI$_3$) and mixed halide (CsPbI$_2$Br)-based PSC are 30 °C and 10^{12} cm^{-3}, respectively. Although this study focused on some key areas of research, analysis of optical and structural properties is not included in this work.

REFERENCES

A. Kojima, K. Teshima, Y. Shirai, T. Miyasaka, *J. Am. Chem. Soc.* **131** No 17, 6050 (2009) https://doi.org/10.1021/ja809598r.

1. F. Giustino, H.J. Snaith, *ACS Energy Lett.* **1** No 6, 1233 (2016) https://doi.org/10.1021/acsenergylett.6b00499.
2. S.D. Stranks, G.E. Eperon, G. Grancini, C. Menelaou, M.J. Alcocer, T. Leijtens, L.M. Herz, A. Petrozza, H. J. Snaith, *Science* **342** No 6156, 341 (2013) https://doi.org/10.1126/science.1243982.
3. W.S. Yang, J.H. Noh, N.J. Jeon, Y.C. Kim, S. Ryu, J. Seo, *Science* **348** No 6240, 1234 (2015) https://doi.org/10.1126/science.aaa9272.
4. W.J. Yin, J.H. Yang, J. Kang, Y. Yan, S.H. Wei, *J. Mat. Chem. A* **3** No 17, 8926 (2015) https://doi.org/10.1039/c4ta05033a.
5. M.G. Ju, M. Chen, Y. Zhou, H.F. Garces, J. Dai, L. Ma, N.P. Padture, X.C. Zeng, *ACS Energy Lett.* **3** No 2, 297 (2018) https://doi.org/10.1021/acsenergylett.7b01167.
6. M. Chen, M.G. Ju, A.D. Carl, Y. Zong, R.L. Grimm, J. Gu, X.C. Zeng, Y. Zhou, N.P. Padture, *Joule* **23** No 3, P558 (2018) https://doi.org/10.1016/j.joule.2018.01.009.
7. K. Chakraborty, M.G. Choudhury, S. Paul, *Sol. Energy* **194** No 12, 886 (2019) https://doi.org/10.1016/j.solener.2019.11.005.
8. S.S. Urmi, et al. *Nanomaterials* **13** No 14, 2100 (2023) https://doi.org/10.3390/nano13142100.
9. A.S. Alali, F. Inaniret, *Nanomaterials* **16** No 5, 324 (2026) https://doi.org/10.3390/nano16050324.
10. N. Rai, S. Rai, P.K. Singh, P. Lohia, D.K. Dwivedi, *J. Mat. Sci: Mat. Elec.* **31** No 8, (2020).
11. K. Chakraborty, S. Paul, U. Mukherjee, S. Das, *J. Nano-Electron. Phys.* **13** No 3, 03009 (2021) https://doi.org/10.21272/jnep.13(3).03009.
12. K. Chakraborty, M.G. Choudhury, S. Paul, *IEEE Trans. Dev. Mat. Reli.* **21** No 4, (2021).
13. K. Tan, P. Lin, G. Wang, Y. Liu, Z. Xu, Y. Lin, *Solid-State Electron.* **126** No 12, 75 (2016) https://doi.org/10.1016/j.sse.2016.09.012.
14. K. Chakraborty, M.G. Choudhury, S. Paul, *IEEE J. Photovolt.* **11** No 2, 386 (2021) https://doi.org/10.1109/JPHOTOV.2021.3050268.
15. N. Chaudhary, R. Chaudhary, *J. Mat. Chem. C* **3** No 45, (2015).
16. Y. Yang, J. You, *Nature* **544** No 4, 155 (2017) https://doi.org/10.1038/544155a.
17. A. Zhang, Y. Chen, J. Yan, *IEEE J. Quan. Elec.* **52** No 6, (2016).
18. Shubham, Raghvendra, C. Pathak, S.K. Pandey, *IEEE Trans. Elec. Dev.* **67** No 7, 2837 (2020) https://doi.org/10.1109/TED.2020.2996570.
19. Pinzon, et al., *Solar* **2**, 559 (2022) https://doi.org/10.3390/solar2040033.

Оптимізація різних фізичних властивостей перовскітного сонячного елемента на основі $CsPbI_{3-X}Br_X$ ($X = 0, 1$)

Kunal Chakraborty[1], R. Narmadha[2], Islom Kadirov[3], Visalakshi Narapareddi[4], M. Lakshmu Naidu[5], Karedla Chitambara Rao[6]

[1] *Department of Electrical Engineering, IMPS College of Engineering and Technology, Malda, West Bengal, India*
[2] *Department of Mechatronics, Sathyabama Institute of Science and Technology, Chennai, Tamil Nadu, India*
[3] *Department of Transport Systems, Urgench State University, Urgench, Uzbekistan*
[4] *School of Business, Aditya University, Aditya Nagar, ADB Rd, 533437 Surampalem, Andhra Pradesh, India*
[5] *Department of Electronics and Communication Engineering, Koneru Lakshmaiah Education Foundation, Vaddeswaram, 522302 Guntur, Andhra Pradesh, India*
[6] *Department of Electronics and Communication Engineering, Aditya Institute of Technology and Management, 532203 Tekkali, Andra Pradesh, India*

Перовскітні сонячні елементи є найперспективнішими альтернативними джерелами чистої енергії. У роботі було розроблено звичайний галогенідний (CsPbI$_3$) та змішаний галогенідний (CsPbI$_2$Br) PSC для дослідження товщини, температури пристрою та щільності дефектів матеріалу за допомогою симулятора SCAPS-1D за ідеальної температури навколишнього середовища 27 °C. У цій моделі пристрою TiO_2 та CuSCN використовуються як ETL (шар переносу електронів) та HTL (шар переносу дірок), а FTO та Ag використовуються як передній та задній електроди відповідно. Структура пристрою – це модель *n-i-p* типу FTO/TiO_2/CsPbI$_3$/CuSCN/Ag та FTO/TiO_2/CsPbI$_2$Br/CuSCN/Ag на основі галогенідів та змішаних галогенідів. Оптимізована товщина PSC на основі галогенідів (CsPbI$_3$) та змішаних галогенідів (CsPbI$_2$Br) становить 500 нм. Оптимальна ефективність перетворення для PSC на основі галогенідів та змішаних галогенідів FTO/TiO_2/CsPbI$_3$/CuSCN/Ag та FTO/TiO_2/CsPbI$_2$Br/CuSCN/Ag становить 11,07 % та 10,89 % відповідно. ЛІОС (летучих органічних сполук) PSC на основі галогенідів (CsPbI$_3$) та змішаних галогенідів (CsPbI$_2$Br) у точці максимальної потужності становить 1,21 В та 0,84 В. Оптимальна температура пристрою та щільність дефектів матеріалу для PSC на основі галогенідів (CsPbI$_3$) та змішаних галогенідів (CsPbI$_2$Br) становлять 30 °C та 1012 см$^{-3}$ відповідно.

Ключові слова: CsPbI$_3$, CsPbI$_2$Br, Перовскіт, SCAPS-1D, Товщина, PCE.